Journal of Materials Chemistry B

ROYAL SOCIETY OF CHEMISTRY

PERSPECTIVE

View Article Online
View Journal | View Issue

Cite this: J. Mater. Chem. B, 2024, 12, 64

Intestinal retentive systems – recent advances and emerging approaches

Durva A. Naik,[a] Spencer Matonis,[a] Gaurav Balakrishnan[a] and Christopher J. Bettinger *[ab]

Received 14th August 2023,
Accepted 15th November 2023

DOI: 10.1039/d3tb01842c

rsc.li/materials-b

Intestinal retentive devices (IRDs) are devices designed to anchor within the lumen of the intestines for long-term residence in the gastrointestinal tract. IRDs can enable impactful medical device technologies including sustained oral drug delivery systems, indwelling sensors, or real-time diagnostics. The design and testing of IRDs present a myriad of challenges, including precise deployment of the device at desired intestinal locations, secure anchoring within the gastrointestinal tract to allow for natural function, and safe removal of the IRD at user-defined times. Advancing the state-of-the-art of IRD is an interdisciplinary effort that requires innovations such as new materials, novel anchoring mechanisms, and medical device design with consistent input from clinical practitioners and end-users. This perspective briefly reviews the current state-of-the-art for IRDs and charts a path forward to inform the design of future concepts. Specifically, this article will highlight materials, retention mechanisms, and test beds to measure the efficacy of IRDs and their mechanisms. Finally, potential synergies between IRD and other medical device technologies are presented to identify future opportunities.

1. Introduction

The gastrointestinal (GI) tract is an exciting testbed for resident medical devices and one that is brimming with innovative research opportunities. Home to over 400 million neurons and 100 trillion microbes, the gut is fundamental to maintaining homeostasis[1,2] through host immunity, endocrine and motor functions, and nutrient absorption.[3] Much like the skin, the gut is a complex organ system with significant surface area for minimally invasive biointeraction, both interventional and diagnostic, with wide-scale potential. GI pathologies severely affect the quality of life of patients and include irritable bowel syndrome (IBS), celiac disease, Crohn's disease, intestinal bleeding, ulcers, *etc.*[4–6] Approximately 45 million people in the US are affected by irritable bowel syndrome (IBS)[7] while Celiac disease[8] and peptic ulcers affect 2 and 4.6 million Americans, respectively, each year.[9] Intestinal retentive devices (IRDs) can leverage the accessibility of the GI tract to offer new paradigms for diagnosing and managing these debilitating diseases.

Gastro-retentive devices have been explored for a range of applications, such as biosensing, weight loss to sustained drug delivery systems for the oral delivery of medications.[10–12] The oral route is the safest and most convenient route for the delivery of medications. However, patient compliance with oral medications drops significantly with the frequency of administration particularly in the case of treating chronic illnesses.[13] Non-compliance causes about 100k premature deaths annually and contributes to over $100B in preventable hospital costs each year.[14–20] Recent advancements in creating long-term gastroretentive medical devices include systems such as the ingestible hydrogel devices developed by Liu *et al.*,[21] ingestible unfolding systems developed by Bellinger *et al.* for malaria elimination,[22] and by Kirtane *et al.* for HIV therapy,[23] and contraceptives.[24] Many of these devices have focused on the delivery of small molecules in the stomach and show favorable pharmacokinetics compared to traditional oral pills but have limited utility in delivering macromolecular therapeutics such as proteins and peptides, which have poor (<1%) oral bioavailability.[25] In comparison, the highly vascularized mucosa in the small intestine makes it an attractive site for drug delivery.[26,27]

As previously referenced, the nervous system of the gut helps coordinate peristalsis and detects and responds to nutrients, hormones, pathogens, and toxins.[28,29] Therefore, there has been a growing interest in the bioelectronics community to develop non-invasive gut-interfacing electronics, which can permit the real-time monitoring of diagnostic indicators as well as the modulated release of therapeutic compounds. Research efforts in resident bioelectronics have been bolstered

[a] Materials Science and Engineering, Carnegie Mellon University, 5000 Forbes Avenue, Wean Hall 3325, Pittsburgh, PA 15213, USA. E-mail: cbetting@andrew.cmu.edu
[b] Biomedical Engineering, Carnegie Mellon University, 5000 Forbes Avenue, Scott Hall 4N201, Pittsburgh, PA 15213, USA

by the progression of miniaturized electronics,[30] biocompatible power supplies,[31–33] wireless power transmission, and novel biosensing pathways.[34,35] Early embodiments of this technology include smart pills such as PillCam, designed to image previously inaccessible diseased tissue sites and reduce the need for more invasive endoscopic procedures.[30,36–38] Additional studies have highlighted the therapeutic benefit of regulating gut microbiota[39] and stimulation of nerve endings in the gut.[40] Nonetheless, there are still significant unmet technical challenges to design, test, and ultimately deploy indwelling ingestible devices including continuous peristalsis,[41] fluctuating fluid volume,[42,43] rapid and dynamic mucus overturn,[44,45] and gradual enzymatic and acidic/basic degradation of devices.[22]

IRD must address several key design challenges: (1) How can devices and associated retention mechanisms be stably ingested and deployed in a timely manner? (2) How can IRD reside within the GI tract while sustaining natural functions? (3) How can devices be removed from the host at the end of their functional lifecycle? This article will discuss the current state-of-the-art for IRDs, present challenges that confront the broad implementation of IRD, and will conclude with materials and device design innovations that could potentially overcome said challenges.

2. Mechanisms of retention

IRDs utilize two primary mechanisms to achieve sustained retention within the gut: chemo-adhesion across the tissue-device interface and mechano-adhesion which uses structural elements of the device that interact with the intestinal epithelium (Fig. 1).

2.1. Chemoadhesion

The intestinal lumen is lined with a lubricious mucus layer, with thickness varying across different sections of the small intestine (based on experiments conducted with the rat intestinal tract), measuring on average 170 μm in the duodenum, 120 μm in the jejunum, and 480 μm in the ileum.[46–48] Mucus is primarily composed of water (>95%) and mucins, which are high-molecular-weight glycoproteins that offer several opportunities to develop mucoadhesive systems.[44,49] Various interactions, such as covalent disulfide bonds between thiomers and cysteine-rich domains of glycoproteins, electrostatic interactions between cationic chitosan and sialic acid moieties, hydrogen bonding, physical entanglements, and van der Waals forces, can generate chemo-adhesive devices.[44,50] Based on the structure of chemo-adhesive devices they can be divided into four categories: (1) mucoadhesive patches, (2) particulate systems (3) magneto-mucoadhesives and (4) gels and *in situ* gelling polymers. In this section, we discuss each of these and provide examples.

2.1.1. Mucoadhesive patches. Mucoadhesive patches are multi-layered devices that consist of a mucoadhesive layer which adheres to the intestinal mucosa, and a water-impermeable backing layer, which confers at least two advantages: (a) it prevents the discharge of loaded drug in the lumen thereby resulting in biased transport of the drug into the mucosa, and (b) it prevents proteolytic enzymes from reaching loaded proteins on the luminal side, thus preserving the drug's effectiveness by avoiding accelerated degradation[51] (Fig. 2a). The adhesive layer often consists of polysaccharides like pectin, Carbopol, chitosan, carboxymethyl cellulose, ethyl cellulose, alginates, and gelatin since they are biocompatible, bioresorbable, and hydrogels by nature.[45,52,53] Taipaleenmäki *et al.* have discussed advancements in polymers for intestinal adhesion at length.[45] Water-impermeable backings are often composed of ethyl cellulose or cellulose acetate.[53,54] For long-term IRDs, one of the most common limitations is premature release due to the constant passage of food and surface fouling caused by the

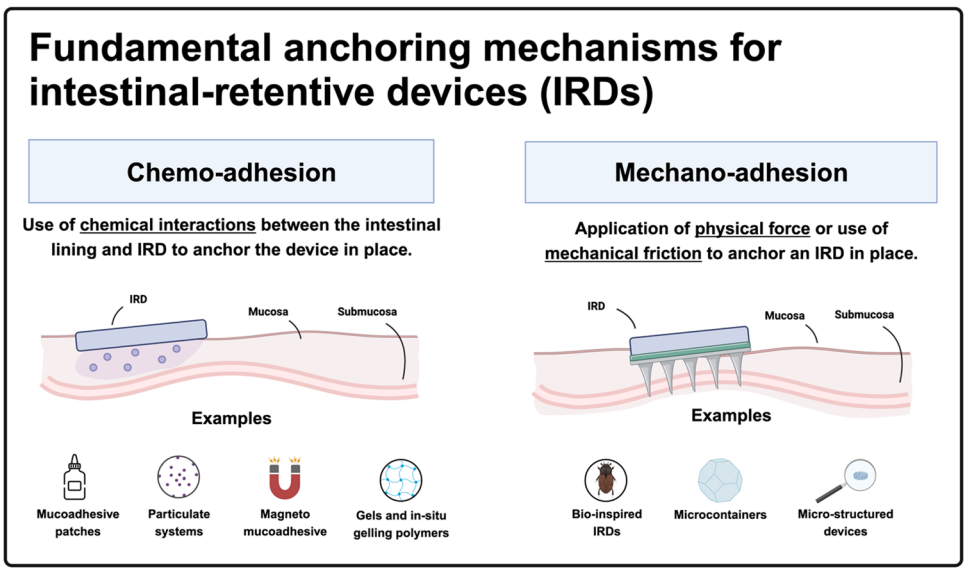

Fig. 1 Summary figure. Infographic outlining the two fundamental anchoring mechanisms for IRDs as well as the seven sub-categories explored in this article (created with BioRender).

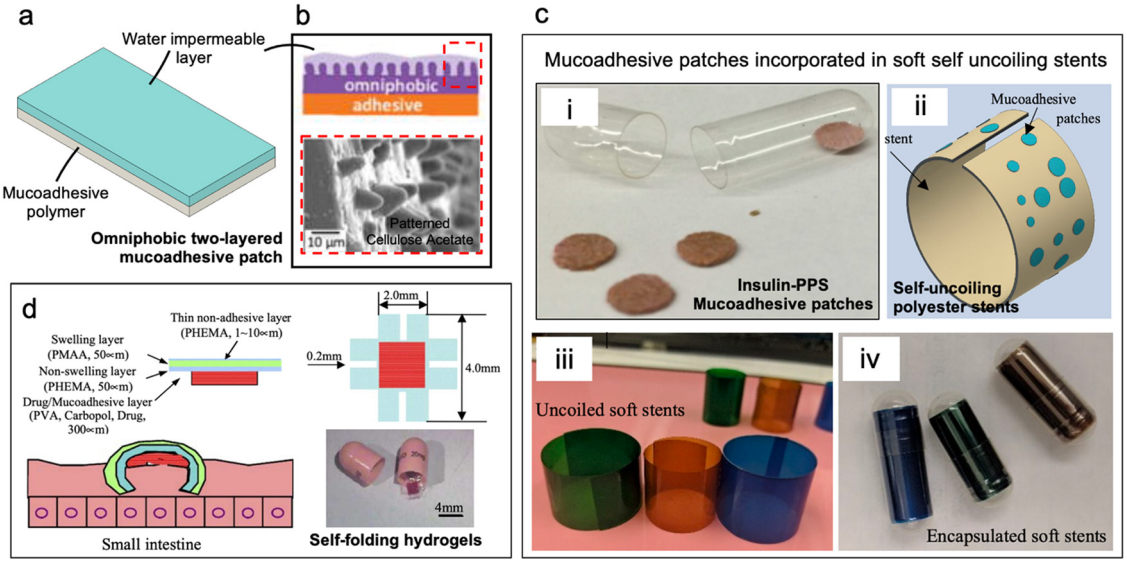

Fig. 2 Mucoadhesive patches. (a) Schematic of a bilayer mucoadhesive patch with a polymeric adhesive layer and a water impermeable backing (b) omniphobic 'Janus' device with a lotus leaf patterned cellulose acetate water-impermeable backing reduces food and protein deposition on mucoadhesive patches. (Reproduced from ref. 54 with permission from Wiley, copyright 2016.) (c) (i) Millimeter-scale mucoadhesive patches containing drug permeation enhancer (dimethyl palmitoyl ammonio propanesulfonate) for oral delivery of insulin. (Reproduced from ref. 53 with permission from Wiley, copyright 2016.) (ii) Patches attached to soft uncoiling polyester stents ease contact of patches to intestinal lumen upon uncoiling. (Reproduced from ref. 61 with permission from ASME, copyright 2021.) (iii) Prototypes of polyester soft stents (iv) stents encased in gelatin capsules for oral delivery. (d) Dual layered self-folding hydrogels with swellable backing layer facilitate hooking onto intestinal mucosa. (Reproduced from ref. 62 with permission from Elsevier, copyright 2006.)

biological fluids contained in the lumen.[55–58] Lee *et al.* solved this issue by introducing structural changes to the water-impermeable cellulose acetate layer to mimic the morphology of lotus leaf, which inherently imparts superhydrophobicity to the leaf, and further chemically functionalized the layer *via* vapor-phase fluorination with perfluorinated silane and then lubricated with a biocompatible, medical-grade perfluorocarbon liquid (Fig. 2b). When used to back Carbopol patches, the modified cellulose acetate backings reduced device interaction with food stuffs and increased the duration of mucosal adhesion of the patches from 7 s to 10 min.[54] Researchers developed tri-layered mucoadhesive patches that include a pH-sensitive layer (*e.g.*, Eudragit polymers L or S). This barrier layer restricts premature drug release in acidic environments of the stomach and thereby allows spatially localized drug delivery to the small intestine. Quatre-layered patches usually distinguish the drug layer and mucoadhesive layer. Detailed reports on the structure of mucoadhesive patches have been reported by Kirsch *et al.*[59] and Sanad *et al.*[60]

Banerjee *et al.* developed ingestible patches to deliver insulin through the intestinal lining for up to 24 h (Fig. 2c(i)).[53] The mucoadhesive patches consisted of small adhesive pellets (diam. = 2–5 mm) comprised of Eudragit E PO, pectin, sodium carboxymethyl cellulose, and dimethyl palmitoyl ammonio propanesulfonate (PPS) to facilitate macromolecules absorption. Orally ingested patches were designed to be retained by fitting into the luminal crevices – anatomical features of the small intestine that can entrap the patches. Sarker *et al.* enhanced the mucoadhesive patches by incorporating them onto the outer layer of polyester-based self-uncoiling stents (Fig. 2c(i–iv)). These stents would automatically uncoil upon reaching the small intestine, allowing the patches to make prompt contact with the intestinal lumen and increase their retention time to approximately 36 h.[61]

Another example of intestinal mucoadhesive patches includes double-coated mucoadhesive films for enhanced delivery of recombinant *Lactococcus lactis*. Here a film of sodium alginate (SA) with an inner coating of Lycoat RS 720 – a hydroxypropyl pea starch – is used to enhance mucoadhesion. Maximum values of mucoadhesion were achieved by 1: (1.1) wt/wt of SA: Lycoat ($\sim$0.098 N cm^{-2}).[63] He *et al.* introduced an innovative mucoadhesive patch that employs self-folding hydrogels (Fig. 2d). The patch contains a bonded bilayer with a finger-like structure and a mucoadhesive drug layer. One layer is pH-sensitive crosslinked poly(methacrylic acid) (PMAA) that swells while the other is poly(hydroxyethyl methacrylate) (PHEMA) and swells significantly less than PMAA. The self-folding device curls due to differential swelling of PMAA:-PHEMA bilayers upon contact with mucus thus improving mucoadhesion and bioavailability with the PHEMA film acting as a barrier layer.[62]

Although mucoadhesive patches show promise for temporary adhesion to improve the oral bioavailability of drugs, they are susceptible to mucus overturn and biofouling which limits their efficacy as a drug delivery system.

2.1.2. Particulate systems. Polymeric particulates represent a distinct class of mucoadhesives that harness materials chemistry and micron-scale dimensions to enhance adhesion.

By maximizing the contact area between the mucoadhesive components of the material, these particulates facilitate their penetration into the mucus membrane and crevices of the intestine. Ponchel *et al.* have provided detailed insights into the mechanism of mucoadhesion of colloidal particulate systems when administered orally in the small intestine.[64] To achieve this purpose, commonly used mucoadhesive polymers like chitosan and sodium alginate are employed to prepare nano/micro-particles or spheres. Ali *et al.* have extensively reviewed the current technology of microspheres for gastroretentive applications.[65] Biodegradable ionomer polymers use electrostatic interactions to promote mucoadhesion. This mechanism however is insufficient when there are large volumes of intestinal fluid and rapid mucus turnover.[64,66] Consequently, researchers are exploring thiolated modifications of particulate systems that induce covalent bond formation between the particles and the cysteine components of the mucosa.[67,68]

Moa *et al.* developed thiol-modified sodium alginate microspheres for sustained drug release in the intestine and in an *in vitro* test demonstrated that thiolation increased the number of retained microspheres by more than 100%.[69] In a separate study, thiolated chitosan particles were investigated for their potential to enhance the absorption of Hesperidin in the intestine for obesity treatment. Although these thiolated particles achieved 6× longer retention times compared to non-thiolated particles, *in vivo* residence times were only 24 h as measured in mice which is comparable to the state-of-the-art.[70]

While particulate systems effectively enhance drug permeation through the intestinal epithelium, they tend to aggregate within the villi and are eventually expelled due to mucus turnover. Consequently, their application as intestinal retentive systems is limited.[25,64]

2.1.3. Magneto-mucoadhesives. Mucoadhesive patches and particles can incorporate magnetic particles to precisely deploy devices within the small intestine and help improve their retention. Liu *et al.* developed an orally delivered polyvinyl alcohol hydrogel matrix doped with neodymium-iron-boron magnets which allowed for the retention of the device in the gut for up to 7 days, facilitated by the presence of an external magnet worn on the abdominal skin (Fig. 3a). Further, it enabled localized deployment of living hydrogels doped with synthetic microbes. Microbe-loaded hydrogels were engineered to enable real-time biosensing and perform diagnostic functions at specific sites within the gut.[71] In another study, researchers developed a tubular mucoadhesive ring using a silicone rubber matrix doped with ferromagnetic particles (Fig. 3b). The ring features a chitosan-glycerol film to enhance mucoadhesion and other capabilities including localized cargo deployment and liquid capsule release. The chitosan-glycerol film played a vital role in inducing strong mucoadhesion between the soft robot and the mucosa, with a normal adhesion force of up to 20 mN observed for a mucus concentration of 5% and a contact time of 10 s.[72] Lee *et al.* developed a magnetically actuated capsule with the ability to hold multiple mucoadhesive patches prepared with mussel-inspired catechol-conjugated chitosan for targeted drug delivery in cancer treatment. The capsule featured a neodymium magnet for movement within the gut using an externally applied magnetic field, along with an actuation system that allowed for the active release of patches at specific sections. The patches themselves contained magnetic microparticles, enabling hyperthermia of cancerous lesions by alternating magnetic forces and facilitating localized drug delivery. This comprehensive system not only provides precise and controlled deployment of drug-loaded patches to targeted gut lesions but also demonstrates the effectiveness and utility of magnetic systems in gastroretentive medical devices.[73]

Incorporating magnetic particles into mucoadhesive colloidal systems can significantly improve their adhesion to the

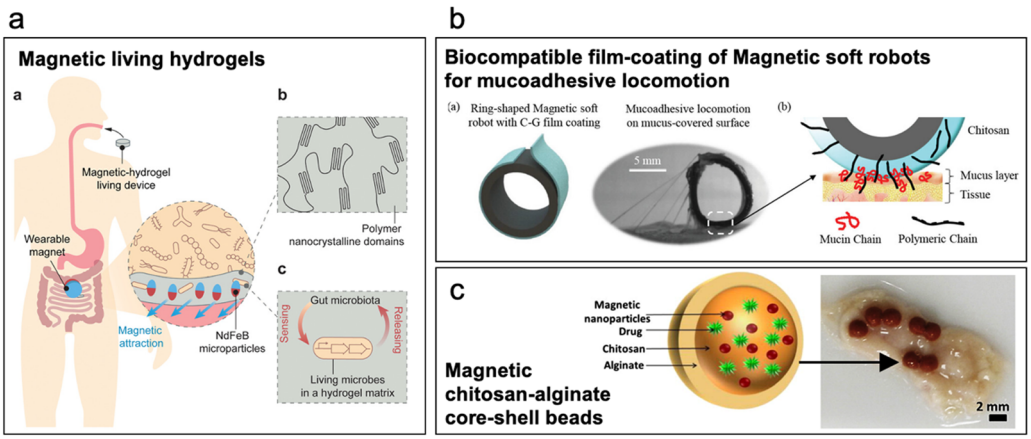

Fig. 3 Magneto-mucoadhesives. (a) Magnetic living hydrogels: PVA hydrogel with NdFeB magnetic microparticles doped with living microbes for real-time biosensing. External magnet is used to retain the hydrogel in the intestine. (Reproduced from ref. 71 with permission from Wiley, copyright 2021.) (b) Tubular silicone-based soft robot is doped with ferromagnetic particles and coated with a chitosan-glycerol film to enhance mucoadhesion to the intestinal mucosa. (Reproduced from ref. 72 with permission from Wiley, copyright 2023.) (c) Magnetic chitosan-alginate core–shell microbeads developed to increase bioavailability of low permeable drugs in presence of external magnetic force. (Reproduced from ref. 74 with permission from Wiley, copyright 2014.)

intestinal lumen when subjected to an external magnetic field. For example, Teply *et al.* utilized negatively charged insulin-doped poly(L-lactic-*co*-glycolic acid) (PLGA) microparticles, which were coupled with positively charged micromagnets to form a complex. Magnetically coupled PLGA microparticles exhibited approximately seven times greater retention compared to non-coupled particles.[75] In another study, Seth *et al.* developed a chitosan-alginate core–shell bead system with magnetic microparticles to increase the residence time and extend the timeline for drug elution thus ultimately improving the bioavailability of drugs with low mucosal permeability (Fig. 3c).[74] Mucoadhesives that employ magnetic materials for retention in the GI tract permit creative avenues for materials design and device concepts. However, many of these concepts use exotic materials which complicate the pathway for regulatory approach. Furthermore, many devices and particles require external devices, complicating deployment and potentially reducing the likelihood of patient compliance, which ultimately may limit the adoption of these devices.

2.1.4. Gels and *in situ* gelling polymers. Gel-based chemo adhesives are materials that encompass *in situ* gelling polymers or pre-gelled polymers. *In situ* gelling polymers react with specific components of the intestine, resulting in the formation of a gel coating on the intestinal surface.[76] Li *et al.* developed an oral solution of *in situ* gelling polymer with dopamine monomers and hydrogen peroxide that polymerize upon reaching the small intestine (Fig. 4a). Catalase concentrations in the small intestine decompose hydrogen peroxide and release oxygen to accelerate polymerization of polydopamine and form a polydopamine coating on the mucosal lining.[77] Polydopamine linings were evaluated for their ability to deliver digestive enzymes, nutrient blockers, and anthelmintic drugs. However, the retention of this coating was found to be limited by mucus turnover. Another example includes therapeutic luminal coatings developed by Lee *et al.* which were made of sucrose octasulfate aluminium complex and engineered into a coacervate formulation linked *via* pH-independent electrostatic interactions. The formulation exhibited hydration and dehydration properties. In the hydrated state, the solid powder transformed into a paste-like substance, allowing for effective and continuous physical coverage of the gastrointestinal mucosa.[78]

Pre-gelled polymers establish interfacial bonds with the intestine upon contact. Examples of pre-gelled intestinal coatings include complex nanoparticle coacervates developed by Zhao *et al.*, which were assembled *via* hydrogen bonding between catechol end groups of the nanoparticles (Fig. 4b). The coacervate adhered to the intestinal lining *via* hydrogen bonding and displayed a retention time of greater than 2 days *in vivo*.[79] Another noteworthy example is the study conducted by Lin *et al.*, where they explored the mucoadhesive properties of nanocellulosic gels. Their findings revealed that the mucoadhesive behavior of these gels varied depending on the type of cellulose used, with different mechanisms of adhesion observed, such as changes in the zeta potential of the

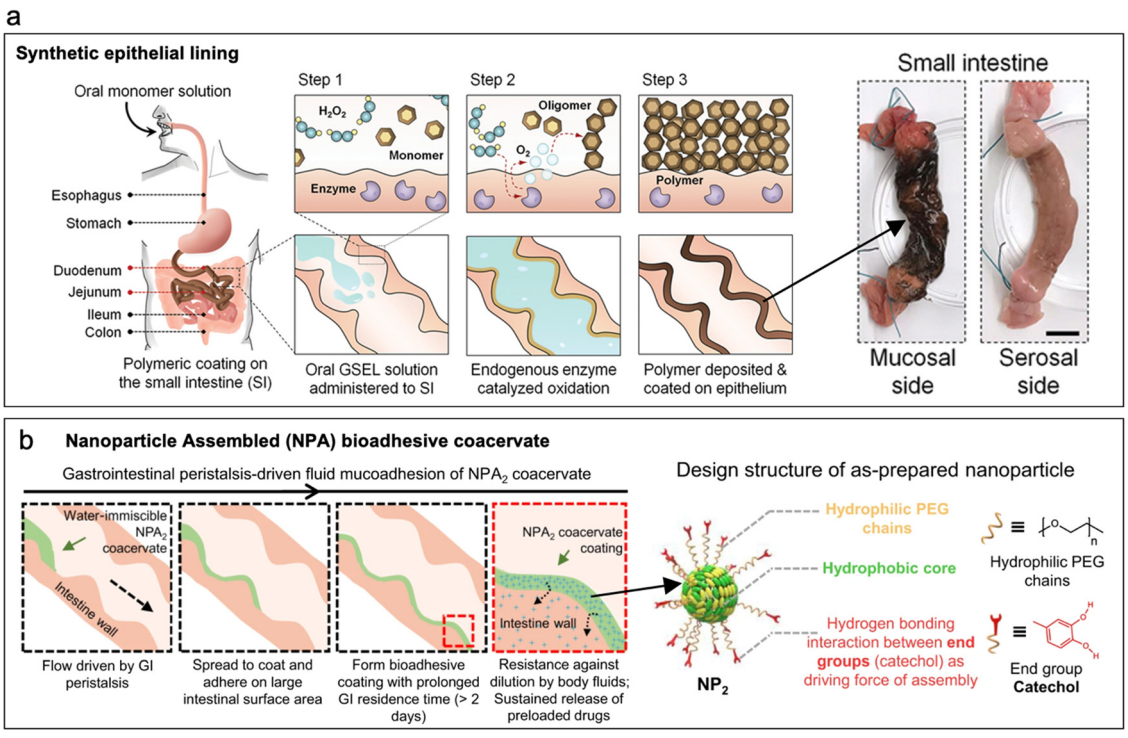

Fig. 4 Gels and *in situ* gelling polymers. (a) Synthetic intestinal epithelial lining produced by enzyme catalyzed *in situ* polymerization of dopamine monomers. (Reproduced from ref. 77 with permission from AAAS, copyright 2020.) (b) Nanoparticle-assembled coacervates are an example of pre-gelled coatings that adhere to intestinal lumen *via* hydrogen bonding between catechol end groups and mucus. (Reproduced from ref. 79 with permission from Nature, copyright 2021.)

cellulose-mucin complex, entanglements, hydrogen bonding, and coagulation.[80]

Gel-based polymeric coatings offer a superior solution for forming a uniform and comprehensive coating on the intricate and convoluted lumen of the intestine.[79] Unlike the mucoadhesive patches, these coatings have the potential to target a larger surface area within the intestine, enabling more effective drug delivery for conditions like inflammatory bowel syndrome.[76,79] However, their retention time is limited to <48 h due to rapid mucus turnover.

2.2. Mechano-adhesion

IRDs can employ mechano-adhesion schemes such as structures that pierce, hook, or otherwise affix to the mucosal lining of the GI tract. These designs may be made of mucoadhesive materials to add a synergistic retention effect. Mechano-adhesives can be distinguished into three broad categories: (1) bio-inspired devices, (2) microcontainers, and (3) micropatterned devices. Here, we discuss these mechanisms and the current state-of-the-art of each of these schemes.

2.2.1. Bio-inspired IRDs. Marine organisms use various mechanisms to achieve underwater adhesion in complex hydrated environments.[81,82] Specifically, octopus and suckerfish have inspired adhesive structures that can be leveraged for intestinal retention.[82–84] Parasitic worms have already won the battle against intestinal barriers and can remain in the intestine for several years if untreated. Inspired by their attachment mechanism, researchers have developed intestinal retentive devices. Inspired by hookworms, Xie *et al.* developed the tissue-attachment mechanism (TAM) which applies microneedles and a vacuum system to mimic the hooks and suction system in hookworms. These devices have shown a record *in vivo* retention time of six days compared to present systems.[85] Inspired by the proboscis of spiny-head worms, Liu *et al.* 3 D printed barbed microneedles which exhibit a pull-out force of 25 mN and a low penetration force of 1.6 mN (Fig. 5a).[86] Building on this mechanism, a spring-microneedle unit was fabricated for integration with pill-based resident systems. Here, the aim was to achieve the required actuation force ($\sim$8 mN) to permit penetration of the barbed microneedles using the spring system.[87] A simple yet effective solution, this mechanism was further incorporated into spiny microneedle anchoring drug deposit (SMAD) and evaluated in *ex vivo* test beds.[88]

Another device inspired by the swellable proboscis of endoparasite *Pomphorhynchus laevis* was developed by Yang *et al.* (Fig. 5b). Here, biphasic conical microneedles with a swellable tip of poly(styrene)-*block*-poly(acrylic acid) (PS-*b*-PAA) and non-swellable polystyrene core were prepared.[89] Minimal insertion force was required to insert said devices into the tissue and post swelling displayed an adhesion force of 4.53 N cm^{-2} with intestinal tissue [this value is for flexible (PS-elastomer) based microneedles]. Yet another device inspired by a parasite – Hookworms – is Theragrippers which are micron-sized devices (250 μm when open, 150 μm when closed) which comprise thick rigid segments and residually stressed bilayer hinges, capped with a thermosensitive wax layer (Fig. 5c).[90] At body temperature the microtips curl up autonomously as the wax softens and pierce the intestinal epithelium to enable retention. These devices show promise as they were retained in rat colon (administered by pneumatic microfluidic controller) and in the upper GI tract of porcine model (administered by endoscopy) for 24 h.

2.2.2. Microcontainers. Size-dependency of sub-micron-sized polystyrene drug carriers on intestinal adhesion has been extensively studied in the treatment of IBS with size inversely

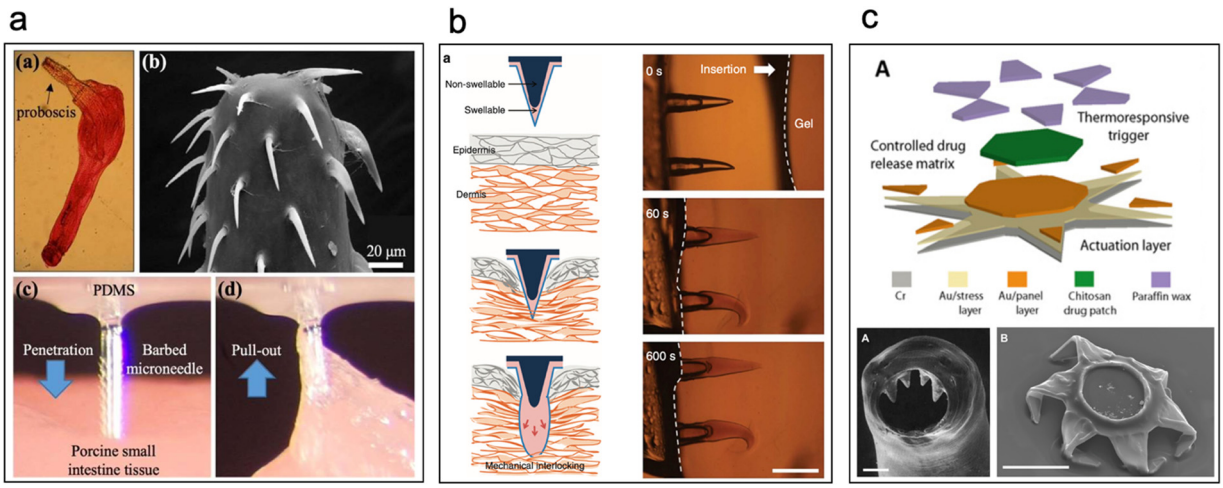

Fig. 5 Bio-inspired IRDs. (a) Barbed microneedles inspired by proboscis of spiny-head worms pierce the intestinal epithelium and hook on to the intestinal mucosa. (Reproduced from ref. 86 with permission from IEEE, copyright 2020.) (b) Biphasic swellable microneedles inspired by swellable proboscis of endoparasite *Pomphorhynchus laevis* enable robust anchoring in the intestine. (Reproduced from ref. 89 with permission from Springer, copyright 2015.) (c) Theragrippers are micron-sized thermosensitive actuators that curl up autonomously due to the internal physiological temperature of the body which facilitates piercing of intestinal epithelium to enable retention. (Reproduced from ref. 90 with permission from Science, copyright 2020.)

related to the binding ability of the particles to mucosa.[91,92] Like mucoadhesive microspheres, these devices, by virtue of their sub-micron-sized shape, can lodge into the crevices of the small intestine and further enter the mucosal layer. Previously, due to the lack of advanced fabrication techniques such as lithography, microfluidics and photopolymerization,[93–95] exclusively microencapsulated containers of spherical shapes were studied. However, with the advent of new fabrication techniques, particles with shapes like plug, vase, toroidal, rods, and cones have been prepared.[92,96–98]

Cylindrical microcontainers with drug loading capacity developed and studied for drug delivery in the small intestine showed a promising increase of 180% oral bioavailability of model drugs like ketoprofen[99] and furosemide.[100] Mosgaard *et al.* further investigated the mucoadhesion of hollow microcontainers of cylindrical and triangular shapes, with varied aspect ratios and materials in an *ex vivo* intestinal perfusion model (Fig. 6a).[101] High-aspect-ratio cylindrical microcontainers comprised of SU-8 adhered more tightly to the mucosa under simulated intestinal fluid flow compared to microcontainers with low aspect ratio cylinders prepared with lightweight polycaprolactone. Furthermore, microcontainers with pyramidal geometries adhered more efficiently to the mid-intestinal section because of their sharp edges which allowed easier penetration into the mucosa. Chrisfort *et al.* further explored the effect of cubic microcontainers and adjunct micropillars on cylindrical containers on colonic mucoadhesion and showed that cubic microcontainers are more efficient in adhering to the mucosa when compared to cylindrical and triangular shaped microcontainers (Fig. 6b). Presence of micropillars did not make a significant impact on adhesion.[102] Based on this technology, radiopaque microcontainers with micropillars and arrows[103] for X-ray diagnostics have been developed. To improve mucoadhesion and retention of microcontainers in the gut, 3D-printed anchor-like surface structures have been studied. The addition of anchors showed a 2× increase in mucoadhesion when compared to nonstructured controls. Branched out surface structure of anchors eased their penetration into the mucosa to interlock the microcontainers within the mucosa (Fig. 6c).[104]

2.2.3. Micropatterned devices. Micropatterned devices resist peristaltic shear in the gut by enhancing friction between intestinal tissue and device substrates. Rose *et al.*[106] provide a detailed overview of prevalent and emerging microfabrication techniques for producing polymeric microstructures. The preferred method for creating micropatterned devices for intestinal retention has been replica molding of microstructures using master molds prepared *via* either photolithography or 3D printing.[107,108]

In a study by Kwon *et al.*, micropatterned silicone-based substrates with low-aspect-ratio microposts of varying diameters and spacings were explored for their adhesion to intestinal tissue (Fig. 7a(i)).[107] The highest frictional force between the substrates and the intestine occurred when the microposts had a diameter of 140 μm (aspect ratio of 0.89 : 1) and a spacing of 75% of the pillar diameter. Furthermore, the friction force was directly proportional to the applied normal force and the viscosity of the surrounding environment between the microposts and the tissue.

Glass *et al.* designed a three-legged anchoring system for an endoscopic capsule to examine its retention in a simulated gut environment.[109] They attached three "legs" (length = 1 cm) with microposts of an aspect ratio of 1 : 1 (diam. = 140 μm; center-to-center dist. = 175 μm) to the capsule (Fig. 7a(ii) and (iii)). An actuating system was incorporated to push the adhesive legs onto the intestinal walls and generate a high-friction interface. The researchers demonstrated that the capsule effectively resisted axial peristaltic shears when the actuating force exceeded 0.27 mN. Additionally, high-viscosity silicone oil-coated microposts increased friction by 400% compared to flat

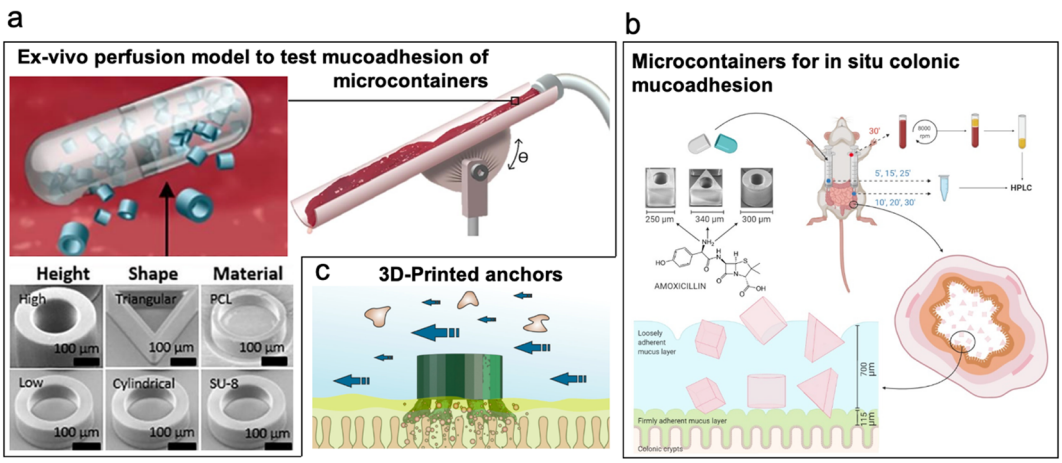

Fig. 6 Microcontainers. (a) Microcontainers with varied structures such as high-aspect-ratio and low-aspect-ratio cylinders and pyramids tested for mucoadhesion *via ex vivo* perfusion model. (Reproduced from ref. 105 with permission from Elsevier, copyright 2019.) (b) Microcontainers (cubic, cylindrical, and pyramid) containing model drug amoxicillin tested for drug delivery in colon. (Reproduced from ref. 102 with permission from MDPI, copyright 2020.) (c) 3D-printed microcontainers with surface textured anchors for enhanced mucoadhesion. (Reproduced from ref. 104 with permission from ACS, copyright 2020.)

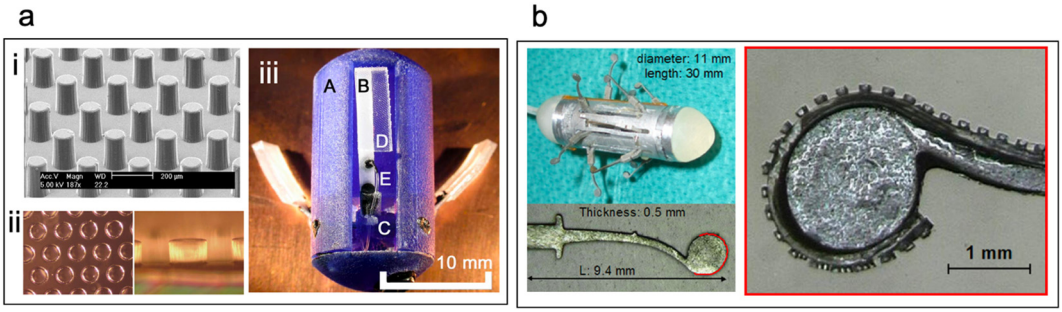

Fig. 7 Micropatterned devices. (a) (i) Silicon-based micropillars for friction enhancement between intestinal mucosa and device substrates. (Reproduced from ref. 107 with permission from IOP, copyright 2006.) (ii) Soft micropillars (aspect ratio 1 : 1) used for three-legged anchoring system for capsule endoscopy (iii) three-legged anchoring system (A) capsule shell, (B) leg, (C) pulley, (D) adhesive pad, (E) cable (Reproduced from ref. 109 with permission from IEEE, copyright 2008.) (b) Nitinol legs with multiple soft-micropillars augment friction in active capsule endoscopy. (Reproduced from ref. 110 with permission from IOP, copyright 2010.)

substrates. Buselli *et al.* developed a capsule with multiple nitinol legs inspired by insects and covered the edges with soft polymeric substrates featuring microposts of varying aspect ratios (Fig. 7b).[110] Their work revealed that, aside from pillar diameter, the material of the microposts and the morphology of the intestinal tissue influenced the friction induced between the microposts and the intestine which is anatomy-dependent. Friction enhancement is valuable for slowing down the transit of endoscopic capsules, but it requires external actuators to ensure proper contact between the microposts and the tissue.

Building on this design concept, Naik *et al.* investigated the interlocking capabilities of micropillars with intestinal villi to withstand peristaltic shear.[108] The study demonstrated that micropillar array patches with micropillar dimensions comparable to intestinal villi effectively penetrated the villi under jejunal contractile pressures and could resist peristaltic shears of up to 0.1 N cm^{-2}. Additionally, computational models were employed to explore various factors influencing the interlocking ability of the micropillars with the villi. These factors included micropillar array pitch, the microposts' tip geometry, the arrangement of the micropillars, and the influence of the micropillars' moduli. The study further showed promising potential for villi-inspired devices to integrate mechanical interlocking and frictional enhancement simultaneously to increase retention time.

3. Current challenges and emerging technologies

3.1. Complexity of intestinal environment

The intestinal environment presents numerous challenges for the effective deployment of active devices. First, the constrictions of the intestine limit the overall device size. Moreover, the intestine is soft, mechanically compliant,[111,112] and coated with the shear-thinning mucus layer that undergoes turnover at a rate comparable to the gut transit time in humans, which spans 24–48 h.[25,113,114] In addition, the intestine undergoes fluctuations in fluid volumes and experiences dynamic peristaltic waves, marked by contractions and varying shear forces.[41,111,115] These conditions, along with the continuous secretion and activity of digestive enzymes can challenge the mechanical integrity of the device.[25] Furthermore, folds in the intestinal lumen can trap device components, leading to obstructions that require surgical removal. Lastly, there is a potential for device displacement due to the movement of the bolus within the intestine, further emphasizing the need for robust device design and secure fixation mechanisms.

Uniform testbeds must be established to evaluate the efficacy of current and emerging IRDs. A summary of retention performance, as previously tabulated by Naik *et al.*,[108] has been extended in Table 1 to encompass additional insights derived from the mechanisms explored within this perspective. Moreover, we have explicitly indicated the model employed to evaluate retention performance. It is noteworthy that a variety of testing strategies have been applied to analyze the retention of intestinal retentive devices, emphasizing the necessity to narrow this range to establish a more standardized technique for evaluating the efficiency of IRDs. While some efforts have been made to evaluate mechano-adhesives through pull-off tests using *ex vivo* intestinal tissues, the testing of mucoadhesives often focuses solely on their ability to adhere to the mucosa.[53] However, the effect of mucus overturn and enzymatic degradation of biodegradable mucoadhesives is often overlooked, with some tests only assessing their performance in simulated gastric fluids.[77] Undoubtedly, initial testing using *in vitro* test beds is justified due to the resource-intensive nature and ethical considerations associated with animal subjects. Nevertheless, there is an urgent need to devise innovative testing strategies that can more accurately simulate the complex intestinal environment encountered by IRD.

Promising inspiration can be drawn from existing models developed for the digestive tract. One such model, devised by Wang *et al.*, features a J-shaped stomach system and a cylindrical small intestine.[116] It incorporates an electromechanical driving instrument comprised of eccentric wheels, rollers, stomach and pyloric extrusion plates, motors, belts, and pulley systems. This driving device simulates natural movement and

Table 1 Summary of current technologies for intestinal retentive devices

Type	Examples	Materials/structure	Testing strategy	Intestinal adhesion or retention performance
Chemoadhesives				
Mucoadhesive patches	Janus omniphobic mucoadhesive devices[54]	Carbopol, microstructured cellulose acetate backing	*Ex vivo* detachment tests and flow model using porcine intestinal mucosa	Janus omniphobic devices improve adhesion to 10 minutes from 7 seconds *vs.* Carbopol adhesives
	Insulin PPS Patches[53]	Eudragit EPO, pectin, sodium carboxymethyl cellulose	*Ex vivo* detachment tests with porcine intestinal mucosa	0.98 mN mm^{-2} (shear adhesion)
	Self-uncoiling stents[61]	Polyester cylinders covered with mucoadhesive patches	Benchtop experiment with simulated peristalsis using excised porcine SI and *in vivo* tests in porcine models	Total retention time ~36 hours *in vivo*
	Double-coated mucoadhesive film[63]	Film prepared with Sodium alginate and Lycoat RS 720	Mucoadhesion tensile test (animal model not specified)	~0.098 N cm^{-2}
	Self-folding device[62]	Folding bilayer: poly (methacrylic acid) poly(hydroxyethyl methacrylate) and mucoadhesive drug depot: PVA, Carbopol	*Ex vivo* detachment tests with simulated fluid flow using porcine intestinal mucosa	Avg. residence time of folded devices was estimated ~1 hour 45 minutes
Particulate systems	Thiol-modified sodium alginate microspheres[69]	Thiol-modified sodium alginate microspheres	*Ex vivo* adherence test using small intestine obtained from Kunming mice	Adherence increases 100% *via* thiolation (absolute adhesion not tested)
	Thiolated chitosan particles[70]	Thiolated chitosan particles	*In vivo* imaging in mice	Maximum retention time 24 hours. Thiolated particles achieve 6× longer retention than non-thiolated particles
Magneto-mucoadhesives	Magnetic living hydrogels[71]	Polyvinyl alcohol hydrogel matrix doped with NdFeB ferromagnetic microparticles	*In vivo* imaging in mice	*In vivo* retention 7 days with wearable magnet intact, 6 hours without magnet
	Tubular mucoadhesive ring[72]	Magnetic silicone tube with glycerol-chitosan coating	*In vitro* test using mucus plate with varying mucus concentrations	~45 mN at preload 20 mN, contact time 10 s, mucus concentration 5%
	Magnetically actuated capsule[73]	Neodymium magnet, mucoadhesive patches: catechol-conjugated chitosan	*Ex vivo* tests performed to evaluate targeted delivery of mucoadhesive patches	—
	Charge-coupled polymeric microparticles and micromagnets[75]	PLGA-based microparticles, Superparamagnetic iron oxide microparticles	*In vitro* flow study (rate 0.8 mL min^{-1}) and *in vivo* retention in mice	Retention time with magnet ~36 hours
	Polymeric microparticles[74]	Core–shell chitosan–alginate Fe_3O_4 incorporated magnetic beads	*Ex vivo* tests on Wistar rats	Tested for 2 hours
Gels and *in situ* gelling polymers	Synthetic epithelium lining[77]	Tissue surface initiated polydopamine coating	Qualitative analysis of adhesion by scrapping lining on polycarbonate	Retention time limited to mucus turnover
	Therapeutic luminal coating[78]	Sucrose octasulfate aluminium complex	*In vitro* test using mucin-coated membranes and *in vivo* tests in rats	Retention time limited to mucus turnover
	Nanoparticle-assembled bioadhesive coacervate coating[79]	Catechol functionalized end groups with polyethylene glycol hydrophilic chains	*In vivo* retention tests in rats	Work of adhesion 7.07 μJ mm^{-2} Retention time ~2 days
	Nano cellulosic gels[80]	Various nano cellulosic gels	*Ex vivo* flow-through tests with porcine intestine	Tested for maximum 10 minutes
Mechanoadhesives				
Bio-inspired IRDs	Tissue attachment mechanism[87]	Sucker teeth of leech and tapeworms	*In vitro* adhesion tests porcine intestinal tissue *In vivo* tests with porcine models	Max adhesion strength 8.09 N per device Retention time 6 days
	Barbed microneedles – tissue anchoring microneedles[86]	Spikes of proboscis of spinyhead worm acanthocephala (later incorporated in spiny microneedle anchoring drug deposit)	*Ex vivo* adhesion tests with porcine intestinal tissue	Max pull-out force 25 mN per microneedle
	Swellable microneedles – biphasic microneedle with swellable tips[89]	Swelling of proboscis of pomphorhynchus laevis	*Ex vivo* adhesion tests with porcine intestinal tissue	Mean adhesion strength 4.53 N cm^{-2}
	Theragrippers[90]	Inspired by Hookworms	*In vivo* adhesion tests in Wistar rat colon and *in vivo* tests in porcine upper GI tract	Retains in both sites for 24 hours, removed naturally by mucosal turnover
Microcontainers	High and low aspect ratio cylindrical, and triangular microcontainers[101]	SU-8 and polycaprolactone-based microcontainers	*Ex vivo* intestinal perfusion model using porcine small intestine	65–81% of microcontainers located at the start of the intestine under perfusion rate of 1.55 mL min^{-1}

Table 1 (*continued*)

Type	Examples	Materials/structure	Testing strategy	Intestinal adhesion or retention performance
	Cubic, cylindrical, triangular, and cylindrical with microposts[102]	SU-8 based microcontainers	Closed-loop colon perfusion study in rats	Cubic microcontainers displayed ~3 times greater retention
	3D printed reservoirs: microcontainers with anchoring adjuncts[104]	DLP 3D printed microcontainers (HTM 140 M V2 3D printing resin)	*Ex vivo* tensile detachment tests with porcine intestinal mucosa and flow retention tests at 4.1–81.9 mL min^{-1} perfusion rate	Addition of anchors showed 2× increase in mucoadhesion when compared to non-structured controls.
Micropatterned devices	Micro-patterned wet adhesives (aspect ratio ~1 : 1)[107] incorporated in tri-legged capsule anchoring system[109] and active capsule endoscopy	Silicone-based 1 : 1 microstructures	*Ex vivo* lap shear tests with porcine intestinal mucosa	0.0828 N cm^{-2} (preload 0.131 N, height 125 μm, diameter 140 μm, edge-to-edge spacing 105 μm, viscosity 10 000 cSt)
	Villi-inspired mechanical interlockers[108]	Silicone based ~1 : 5 microstructures	Mechanical simulations, *in vitro* analyses and *ex vivo* tests with porcine intestinal mucosa	Simulations predict interlocking can resist shear of 0.1 N cm^{-2}, *ex vivo* tests reveal ~1.4 mN mm^{-2}

peristaltic contractions in the stomach and duodenum. Deng *et al.* constructed a soft tubular model equipped with artificial villi, which simulates peristalsis *via* a homemade cross-shaped rotating device which periodically pushes the shaft onto the tube using a stepped motor to simulate contractions.[117,118] This model proves valuable for testing the residence time of fluid particles in the intestine and can be adapted for assessing the residence time of devices. Wu *et al.* have authored an insightful article that consolidates various developed models for digestive tracts.[119] Their work serves as a comprehensive resource, providing inspiration for the construction of large-scale three-dimensional intestinal models. By leveraging the knowledge and approaches derived from these existing models, researchers can construct sophisticated 3D intestinal models that faithfully replicate the intricate dynamics of the intestine. These models facilitate more realistic testing of IRDs, taking into account crucial factors such as peristalsis, fluid volumes, luminal restrictions, and anatomical variations within the intestine.

Computational modeling of intestinal fluid flow volumes can permit the evaluation of device retention mechanisms in the gut under varying volume conditions.[120,121] Additionally, finite element analysis has been effectively employed to assess the penetration capacity of mechano-adhesive gastroretentive devices, such as theragrippers[90] and kirigami-inspired stents,[122] designed for targeted local delivery of therapeutics. These computational techniques allow for the incorporation of diverse morphological conditions, considering factors like patients' age and the specific section within the small intestine.

Gut-on-a-chip systems are another platform that can accelerate device testing.[123] These systems can simulate *in vivo* fluidic flow, peristalsis-like motions, host-microbe crosstalk, and multi-cell type interactions, making them highly valuable for personalized medicine applications. Noteworthy contributions to this area of research can be found in the works of Xiang *et al.*[124] and Thomas *et al.*,[125] who have provided detailed discussions on gut-on-a-chip *in vitro* models. Additionally, several *in vitro* models have been specifically designed to replicate the presence of mucus in the gut, offering accurate and controlled testing environments for mucoadhesive devices.[126–128] By incorporating computational analysis, gut-on-a-chip systems, and specialized *in vitro* models, researchers can advance the field of IRDs by improving testing methodologies, optimizing device designs, and ultimately facilitating the development of more effective and patient-specific IRDs.

3.2. Path to clinical translation of intestinal retentive devices

Regulatory approval for commercial IRD products will be performed on a case-by-case basis with attention to their risk-reward profile. Prominent risks for these systems include intestinal perforation, occlusion, device migration, and fibrosis within the GI tract. Unsurprisingly, many of these complications have been documented in relation to GI stents, which clinicians use to alleviate obstructions, mitigate post-operative leaking, and facilitate gastrointestinal bypasses.[129–131] So how can the potential benefit of technologies that use IRD be maximized while minimizing risk to the patient?

The risk of obstruction can be minimized by fabricating devices out of bioresorbable materials that reduce the likelihood of persistent obstruction or occlusion.[132–135] As demonstrated by Bellinger *et al.*, in cases where fully bioresorbable structures are not an option, strategic structural joints may be designed for degradation to compromise structural integrity and enable device motility.[22] Special attention should be given to the anatomical limitations of the pylorus, ileocecal valve, cecum, and anus for safe passage of IRDs descending from the upper bowel.[136] Compared to surgical implants, cytocompatibility of IRD materials poses less of a challenge due to the protective barrier of the intestinal lumen and toughened endothelial cells, however many of the same guidelines apply.[137–139] Avoiding a microneedle penetration depth greater than 3 mm in the small intestine and greater than 1 mm in the large intestine can avoid harmful perforation of the bowel wall.[140–143] These exact guidelines can vary depending on tissue condition, IRD location, and needle characteristics.[144]

The use of soft and compliant materials reduces the likelihood of perforation and bioresorbable elastomers such as poly(glycerol-*co*-sebacate) (PGS), poly(1,3-diamino-2-propanol-*co*-polyol sebacate) (APS), bis-urea-modified polycarbonate (PC-BU), among others can be better leveraged for IRD design.[145–148] Crosslinked hydrogel systems are another favorable candidate with tunable mechanical properties, demonstrated extensively in tissue engineering and drug delivery research. Alginate, collagen, polysaccharide-based structures have been shown to survive *in vivo* environments for up to 7 days but still fall well short of the life spans of synthetic polymers such as polyglycolic acid (PGA), (PLGA), polylactic acid (PLA) and polycaprolactone (PCL) that have been used extensively as structural materials in other contexts.

What happens when an IRD needs to be extracted? Even fully bioresorbable structures may require early retrieval due to an adverse patient reaction or delayed complication. In many cases, manual retrieval will be performed endoscopically using biopsy forceps or specialized grippers. Devices lodged into the submucosa can be lifted from the membrane using a fluidized submucosal injection, as is used for the removal of polyps.[149] In the case of microscale devices, researchers may consider implementing pre-designed points of structural failure to ensure IRD fragments are passed by the patient without irritation. Similarly, structural separation of a therapeutic payload from the anchoring body may be a way to terminate further drug delivery more easily in the case of an emergency. Small devices can leverage fluorescent or radiopaque markers to assist in device location following migration or tissue overgrowth. Mucoadhesive device designers should consider reversible chemical adhesion mechanisms that can be triggered using benign oral agents.[150] In extreme cases, clinicians may resort to endoscopic laser therapy to ablate an anchored IRD out of position, trigger a thermally-reversible adhesion agent[151,152] or use specialized gripping tools such as the Roth net or Dormia basket.

4. Conclusions and future outlook

IRDs hold significant promise in enabling a class of low-profile medical devices with wide-ranging applications such as long-term drug delivery platforms, continuous health monitoring, and non-invasive neuromodulation. A major challenge is designing devices that can achieve programmable non-obstructive device retention within the intestinal tract. This article presents the current state-of-the-art, opportunities, and challenges pertaining to the design of intestinal retentive medical systems.

Historically, most IRDs have been designed with drug delivery applications that allow for small-area interfaces such as particulates, patches, and capsules. As the application space of ingestible and intestinal medical devices continues to expand beyond drug delivery, there will be a need to construct strategies to design large-area interfaces as IRDs. Moving forward, there is an opportunity to leverage advances in shape memory materials,[153,154] rapidly expanding stimuli-responsive materials,[21,155] origami and kirigami-based expanding structures, and *in situ* self-assembling systems to accelerate the progress in functional and large-area IRDs. There is also an opportunity to utilize combinatorial approaches that optimize synergy between mechanical and chemical-based adhesives. While these innovations present a future-forward perspective, the fundamental challenge remains in ensuring effective and lasting adhesion within the intestinal environment.

From chemical to mechanical approaches for adhesion, it is clear that there are several distinct pathways to achieving intestinal retention. Each device application, depending on the size of the deployed structure and desired retention time, will require application-specific strategies to achieve the desired outcome. Intestinal retentive devices could leverage advances in bioelectronics, neuroengineering, soft robotics, and materials chemistry to design unique next-generation ingestible devices that can diagnose and treat a variety of diseases within the gastrointestinal tract.[30,156–159]

Additionally, considering patient risk-benefit and regulatory pathways during the early stages of development can accelerate the translation of intestinal retentive devices from lab to clinic. This foresight in development, combined with technological advancements, positions intestinal retentive devices as a cornerstone in the future of precision medicine and healthcare innovation.

Conflicts of interest

There are no conflicts to declare.

Acknowledgements

The authors acknowledge funding for this article from the National Institute of Biomedical Imaging, and Bioengineering (Grant no. R21EB026073).

References

1 R. Sender, S. Fuchs and R. Milo, *PLoS Biol.*, 2016, **14**, e1002533.
2 M. Million and M. Larauche, *Neurogastroenterol. Motil.*, 2016, **28**, 1283–1289.
3 D. M. Denbow, in *Sturkie's Avian Physiology*, ed. C. G. Scanes, Academic Press, San Diego, 6th Edn, 2015, pp. 337–366.
4 M. Augustyn, I. Grys and M. Kukla, *Clin. Exp. Hepatol.*, 2019, **5**, 1–10.
5 A. B. R. Thomson, *Best Pract. Res., Clin. Gastroenterol.*, 2009, **23**, 861–874.
6 J. Zhan, *WJG*, 2004, **10**, 2585.
7 R. S. Choung and G. R. Locke, *Clin. Gastroenterol.*, 2011, **40**, 1–10.
8 C. Catassi, S. Gatti and E. Lionetti, *Digital Discovery*, 2015, **33**, 141–146.

9 J. H. Kurata and B. M. Haile, *Clin. Gastroenterol.*, 1984, **13**, 289–307.
10 Y.-C. Chen, H.-O. Ho, T.-Y. Lee and M.-T. Sheu, *Int. J. Pharm.*, 2013, **441**, 162–169.
11 Y. L. Kong, X. Zou, C. A. McCandler, A. R. Kirtane, S. Ning, J. Zhou, A. Abid, M. Jafari, J. Rogner, D. Minahan, J. E. Collins, S. McDonnell, C. Cleveland, T. Bensel, S. Tamang, G. Arrick, A. Gimbel, T. Hua, U. Ghosh, V. Soares, N. Wang, A. Wahane, A. Hayward, S. Zhang, B. R. Smith, R. Langer and G. Traverso, *Adv. Mater. Technol.*, 2019, **4**, 1800490.
12 H. Shirin, V. Richter, S. Matalon, D. Abramowich, A. Maliar, E. Shachar, S. F. Moss and E. Broide, *Obes. Sci. Pract.*, 2019, **5**, 376–382.
13 C. I. Coleman, B. Limone, D. M. Sobieraj, S. Lee, M. S. Roberts, R. Kaur and T. Alam, *JMCP*, 2012, **18**, 527–539.
14 C. M. Hughes, *Drugs Aging*, 2004, **21**, 793–811.
15 F. Kleinsinger, *Perm. j.*, 2018, **22**, 18–033.
16 L. Osterberg and T. Blaschke, *N. Engl. J. Med.*, 2005, **353**, 487–497.
17 R. McCarthy, *Bus Health*, 1998, **16**, 27–28.
18 J. S. Berg, J. Dischler, D. J. Wagner, J. J. Raia and N. Palmer-Shevlin, *Ann. Pharmacother.*, 1993, **27**, S1–S24.
19 G. Levy, M. K. Zamacona and W. J. Jusko, *Clin. Pharmacol. Ther.*, 2000, **68**, 586–591.
20 P. J. McDonnell and M. R. Jacobs, *Ann. Pharmacother.*, 2002, **36**, 1331–1336.
21 X. Liu, C. Steiger, S. Lin, G. A. Parada, J. Liu, H. F. Chan, H. Yuk, N. V. Phan, J. Collins, S. Tamang, G. Traverso and X. Zhao, *Nat. Commun.*, 2019, **10**, 493.
22 A. M. Bellinger, M. Jafari, T. M. Grant, S. Zhang, H. C. Slater, E. A. Wenger, S. Mo, Y.-A. L. Lee, H. Mazdiyasni, L. Kogan, R. Barman, C. Cleveland, L. Booth, T. Bensel, D. Minahan, H. M. Hurowitz, T. Tai, J. Daily, B. Nikolic, L. Wood, P. A. Eckhoff, R. Langer and G. Traverso, *Sci. Transl. Med.*, 2016, **8**, 365ra157.
23 A. R. Kirtane, O. Abouzid, D. Minahan, T. Bensel, A. L. Hill, C. Selinger, A. Bershteyn, M. Craig, S. S. Mo, H. Mazdiyasni, C. Cleveland, J. Rogner, Y.-A. L. Lee, L. Booth, F. Javid, S. J. Wu, T. Grant, A. M. Bellinger, B. Nikolic, A. Hayward, L. Wood, P. A. Eckhoff, M. A. Nowak, R. Langer and G. Traverso, *Nat. Commun.*, 2018, **9**, 2.
24 A. R. Kirtane, T. Hua, A. Hayward, A. Bajpayee, A. Wahane, A. Lopes, T. Bensel, L. Ma, F. Z. Stanczyk, S. Brooks, D. Gwynne, J. Wainer, J. Collins, S. M. Tamang, R. Langer and G. Traverso, *Sci. Transl. Med.*, 2019, **11**, eaay2602.
25 T. D. Brown, K. A. Whitehead and S. Mitragotri, *Nat. Rev. Mater.*, 2020, **5**, 127–148.
26 J. T. Collins, A. Nguyen and M. Badireddy, *StatPearls*, StatPearls Publishing, Treasure Island (FL), 2020.
27 P. Kahai, P. Mandiga, C. J. Wehrle and S. Lobo, *StatPearls*, StatPearls Publishing, Treasure Island (FL), 2022.
28 J. Bernier-Latmani and T. V. Petrova, *Nat. Rev. Gastroenterol. Hepatol.*, 2017, **14**, 510–526.
29 B. G. Nezami and S. Srinivasan, *Curr. Gastroenterol. Rep.*, 2010, **12**, 358–365.
30 K. Nan, V. R. Feig, B. Ying, J. G. Howarth, Z. Kang, Y. Yang and G. Traverso, *Nat. Rev. Mater.*, 2022, **7**, 908–925.
31 A. Khademhosseini, C. Bettinger, J. M. Karp, J. Yeh, Y. Ling, J. Borenstein, J. Fukuda and R. Langer, *J. Biomater. Sci., Polym. Ed.*, 2006, **17**, 1221–1240.
32 N. Van Helleputte, A. J. G. Even, F. Leonardi, S. Stanzione, M. Song, C. Garripoli, W. Sijbers, Y.-H. Liu and C. Van Hoof, *J. Microelectromech. Syst.*, 2020, **29**, 645–652.
33 P.-M. Wang, G. Dubrovsky, J. C. Y. Dunn, Y.-K. Lo and W. Liu, *Micromachines*, 2019, **10**, 525.
34 D. Rodrigues, A. I. Barbosa, R. Rebelo, I. K. Kwon, R. L. Reis and V. M. Correlo, *Biosensors*, 2020, **10**, 79.
35 J. Li, J. Y. Liang, S. J. Laken, R. Langer and G. Traverso, *Trends Chem.*, 2020, **2**, 319–340.
36 M. Yu, *Gastroenterology Nursing*, 2002, **25**, 24–27.
37 C. Ell, S. Remke, A. May, L. Helou, R. Henrich and G. Mayer, *Endoscopy*, 2002, **34**, 685–689.
38 G. Ciuti, A. Menciassi and P. Dario, *IEEE Rev. Biomed. Eng.*, 2011, **4**, 59–72.
39 N. C. Knox, J. D. Forbes, G. Van Domselaar and C. N. Bernstein, *Curr. Treatm. Opt. Gastro.*, 2019, **17**, 115–126.
40 R. H. Howland, *Curr. Behav. Neurosci. Rep.*, 2014, **1**, 64–73.
41 R. Kant Avvari, in *Digestive System - Recent Advances*, ed. X. Qi and S. Koruth, IntechOpen, 2020.
42 C. Schiller, C.-P. Frohlich, T. Giessmann, W. Siegmund, H. Monnikes, N. Hosten and W. Weitschies, *Aliment. Pharmacol. Ther.*, 2005, **22**, 971–979.
43 M. W. Klinge, N. Sutter, E. B. Mark, A.-M. Haase, P. Borghammer, V. Schlageter, S. Lund, J. Fleischer, K. Knudsen, A. M. Drewes and K. Krogh, *J. Neurogastroenterol. Motil.*, 2021, **27**, 390–399.
44 G. S. Asane, S. A. Nirmal, K. B. Rasal, A. A. Naik, M. S. Mahadik and Y. M. Rao, *Drug Dev. Ind. Pharm.*, 2008, **34**, 1246–1266.
45 E. Taipaleenmäki and B. Städler, *Macromol. Biosci.*, 2020, **20**, 1900342.
46 C. Atuma, V. Strugala, A. Allen and L. Holm, *Am. J. Physiol.: Gastrointest. Liver Physiol.*, 2001, **280**, G922–G929.
47 L. M. Ensign, R. Cone and J. Hanes, *Adv. Drug Delivery Rev.*, 2012, **64**, 557–570.
48 X. Murgia, B. Loretz, O. Hartwig, M. Hittinger and C.-M. Lehr, *Adv. Drug Delivery Rev.*, 2018, **124**, 82–97.
49 J. Hombach and A. Bernkop-Schnürch, in *Drug Delivery*, ed. M. Schäfer-Korting, Springer Berlin Heidelberg, Berlin, Heidelberg, 2010, vol. 197, pp. 251–266.
50 G. P. Andrews, T. P. Laverty and D. S. Jones, *Eur. J. Pharm. Biopharm.*, 2009, **71**, 505–518.
51 S. Eiamtrakarn, Y. Itoh, J. Kishimoto, Y. Yoshikawa, N. Shibata, M. Murakami and K. Takada, *Biomaterials*, 2002, **23**, 145–152.
52 T. M. Ways, W. Lau and V. Khutoryanskiy, *Polymers*, 2018, **10**, 267.
53 A. Banerjee, J. Lee and S. Mitragotri, *Bioeng. Transl. Med.*, 2016, **1**, 338–346.
54 Y.-A. L. Lee, S. Zhang, J. Lin, R. Langer and G. Traverso, *Adv. Healthcare Mater.*, 2016, **5**, 1141–1146.

55 N. A. Peppas, J. B. Thomas and J. McGinty, *J. Biomater. Sci., Polym. Ed.*, 2009, **20**, 1–20.
56 G. D. Bixler and B. Bhushan, *Philos. Trans. R. Soc., A*, 2012, **370**, 2381–2417.
57 B. Mizrahi, X. Khoo, H. H. Chiang, K. J. Sher, R. G. Feldman, J.-J. Lee, S. Irusta and D. S. Kohane, *Langmuir*, 2013, **29**, 10087–10094.
58 R. G. Nuzzo, *Nat. Mater.*, 2003, **2**, 207–208.
59 K. Kirsch, U. Hanke and W. Weitschies, *Eur. J. Pharm. Biopharm.*, 2017, **114**, 135–144.
60 W. G. Sanad and S. N. Abd-Alhammid, *Eur. J. Mol. Clin. Med.*, 2020, **7**(2), 23–30.
61 S. Sarker, R. Jones, G. Chow and B. Terry, in *2021 Design of Medical Devices Conference*, American Society of Mechanical Engineers, Minneapolis, MN, USA, 2021, p. V001T12A010.
62 H. He, J. Guan and J. L. Lee, *J. Controlled Release*, 2006, **110**, 339–346.
63 E. W. Tan, K. Y. Tan, L. V. Phang, P. V. Kumar and L. L. A. In, *PLoS One*, 2019, **14**, e0219912.
64 G. Ponchel, M.-J. Montisci, A. Dembri, C. Durrer and D. Duchêne, *Eur. J. Pharm. Biopharm.*, 1997, **44**, 25–31.
65 J. Ali, S. Baboota, R. Khar, S. Md, J. Sahni, G. Singh and A. Ahuja, *Syst. Rev. Pharm.*, 2012, **3**, 4.
66 D. Teutonico, S. Montanari and G. Ponchel, *Int. J. Pharm.*, 2011, **413**, 87–92.
67 I. Bravo-Osuna, C. Vauthier, A. Farabollini, G. F. Palmieri and G. Ponchel, *Biomaterials*, 2007, **28**, 2233–2243.
68 V. M. Leitner, G. F. Walker and A. Bernkop-Schnürch, *Eur. J. Pharm. Biopharm.*, 2003, **56**, 207–214.
69 X. Mao, X. Li, W. Zhang, L. Yuan, L. Deng, L. Ge, C. Mu and D. Li, *ACS Appl. Bio Mater.*, 2019, **2**, 5810–5818.
70 T.-C. Chen, Y.-Y. Ho, R.-C. Tang, Y.-C. Ke, J.-N. Lin, I.-H. Yang and F.-H. Lin, *Nutrients*, 2021, **13**, 4405.
71 X. Liu, Y. Yang, M. E. Inda, S. Lin, J. Wu, Y. Kim, X. Chen, D. Ma, T. K. Lu and X. Zhao, *Adv. Funct. Mater.*, 2021, **31**, 2010918.
72 C. Wang, A. Mzyk, R. Schirhagl, S. Misra and V. K. Venkiteswaran, *Adv. Mater. Technol.*, 2023, **8**, 2201813.
73 J. Lee, D. Kim, S. Bang and S. Park, *Adv. Intell. Syst.*, 2022, **4**, 2100203.
74 A. Seth, D. Lafargue, C. Poirier, J.-M. Péan and C. Ménager, *Eur. J. Pharm. Biopharm.*, 2014, **88**, 374–381.
75 B. A. Teply, R. Tong, S. Y. Jeong, G. Luther, I. Sherifi, C. H. Yim, A. Khademhosseini, O. C. Farokhzad, R. S. Langer and J. Cheng, *Biomaterials*, 2008, **29**, 1216–1223.
76 M. Tenci, S. Rossi, V. Giannino, B. Vigani, G. Sandri, M. C. Bonferoni, M. Daglia, L. M. Longo, C. Macelloni and F. Ferrari, *Pharmaceutics*, 2019, **11**, 611.
77 J. Li, T. Wang, A. R. Kirtane, Y. Shi, A. Jones, Z. Moussa, A. Lopes, J. Collins, S. M. Tamang, K. Hess, R. Shakur, P. Karandikar, J. S. Lee, H.-W. Huang, A. Hayward and G. Traverso, *Sci. Transl. Med.*, 2020, **12**, eabc0441.
78 Y. Lee, T. E. Deelman, K. Chen, D. S. Y. Lin, A. Tavakkoli and J. M. Karp, *Nat. Mater.*, 2018, **17**, 834–842.
79 P. Zhao, X. Xia, X. Xu, K. K. C. Leung, A. Rai, Y. Deng, B. Yang, H. Lai, X. Peng, P. Shi, H. Zhang, P. W. Y. Chiu and L. Bian, *Nat. Commun.*, 2021, **12**, 7162.
80 Y.-J. Lin, J. A. Shatkin and F. Kong, *Carbohydr. Polym.*, 2019, **210**, 157–166.
81 A. Mahdavi, L. Ferreira, C. Sundback, J. W. Nichol, E. P. Chan, D. J. D. Carter, C. J. Bettinger, S. Patanavanich, L. Chignozha, E. Ben-Joseph, A. Galakatos, H. Pryor, I. Pomerantseva, P. T. Masiakos, W. Faquin, A. Zumbuehl, S. Hong, J. Borenstein, J. Vacanti, R. Langer and J. M. Karp, *Proc. Natl. Acad. Sci. U. S. A.*, 2008, **105**, 2307–2312.
82 S. Baik, J. Kim, H. J. Lee, T. H. Lee and C. Pang, *Adv. Sci.*, 2018, **5**, 1800100.
83 G. Meloni, O. Tricinci, A. Degl'Innocenti and B. Mazzolai, *Sci. Rep.*, 2020, **10**, 15480.
84 Y. Wang, X. Yang, Y. Chen, D. K. Wainwright, C. P. Kenaley, Z. Gong, Z. Liu, H. Liu, J. Guan, T. Wang, J. C. Weaver, R. J. Wood and L. Wen, *Sci. Robot.*, 2017, **2**, eaan8072.
85 W. Xie, V. Kothari and B. S. Terry, *Biomed. Microdevices*, 2015, **17**, 68.
86 S. Liu, S. Chu, G. E. Banis, L. A. Beardslee and R. Ghodssi, *2020 IEEE 33rd International Conference on Micro Electro Mechanical Systems (MEMS)*, IEEE, Vancouver, BC, Canada, 2020, pp. 885–888.
87 S. Liu, S. Chu, L. A. Beardslee and R. Ghodssi, *J. Microelectromech. Syst.*, 2020, **29**, 706–712.
88 J. A. Levy, M. A. Straker, J. M. Stine, L. A. Beardslee, V. Borbash and R. Ghodssi, *Adv. Mater. Technol.*, 2023, **8**, 2201365.
89 S. Y. Yang, E. D. O'Cearbhaill, G. C. Sisk, K. M. Park, W. K. Cho, M. Villiger, B. E. Bouma, B. Pomahac and J. M. Karp, *Nat. Commun.*, 2013, **4**, 1702.
90 A. Ghosh, L. Li, L. Xu, R. P. Dash, N. Gupta, J. Lam, Q. Jin, V. Akshintala, G. Pahapale, W. Liu, A. Sarkar, R. Rais, D. H. Gracias and F. M. Selaru, *Sci. Adv.*, 2020, **6**, eabb4133.
91 A. Lamprecht, U. Schäfer and C. Lehr, *Pharm. Res.*, 2001, **18**, 788–793.
92 J. A. Champion, Y. K. Katare and S. Mitragotri, *J. Controlled Release*, 2007, **121**, 3–9.
93 S. Xu, Z. Nie, M. Seo, P. Lewis, E. Kumacheva, H. A. Stone, P. Garstecki, D. B. Weibel, I. Gitlin and G. M. Whitesides, *Angew. Chem.*, 2005, **117**, 734–738.
94 D. Dendukuri, D. C. Pregibon, J. Collins, T. A. Hatton and P. S. Doyle, *Nat. Mater.*, 2006, **5**, 365–369.
95 J. P. Rolland, B. W. Maynor, L. E. Euliss, A. E. Exner, G. M. Denison and J. M. DeSimone, *J. Am. Chem. Soc.*, 2005, **127**, 10096–10100.
96 O. D. Velev, A. M. Lenhoff and E. W. Kaler, *Science*, 2000, **287**, 2240–2243.
97 P. Sozzani, S. Bracco, A. Comotti, R. Simonutti, P. Valsesia, Y. Sakamoto and O. Terasaki, *Nat. Mater.*, 2006, **5**, 545–551.
98 J. A. Champion and S. Mitragotri, *Proc. Natl. Acad. Sci. U. S. A.*, 2006, **103**, 4930–4934.

99 L. H. Nielsen, A. Melero, S. S. Keller, J. Jacobsen, T. Garrigues, T. Rades, A. Müllertz and A. Boisen, *Int. J. Pharm.*, 2016, **504**, 98–109.
100 C. Mazzoni, F. Tentor, S. A. Strindberg, L. H. Nielsen, S. S. Keller, T. S. Alstrøm, C. Gundlach, A. Müllertz, P. Marizza and A. Boisen, *J. Controlled Release*, 2017, **268**, 343–351.
101 M. Dalskov Mosgaard, S. Strindberg, Z. Abid, R. Singh Petersen, L. Højlund Eklund Thamdrup, A. Joukainen Andersen, S. Sylvest Keller, A. Müllertz, L. Hagner Nielsen and A. Boisen, *Int. J. Pharm.*, 2019, **570**, 118658.
102 J. F. Christfort, A. J. Guillot, A. Melero, L. H. E. Thamdrup, T. M. Garrigues, A. Boisen, K. Zór and L. H. Nielsen, *Pharmaceutics*, 2020, **12**, 355.
103 T. Chang, R. B. Kjeldsen, J. F. Christfort, E. M. Vila, T. S. Alstrøm, K. Zór, E. Hwu, L. H. Nielsen and A. Boisen, *Adv. Healthcare Mater.*, 2023, **12**, 2201897.
104 L. Vaut, J. J. Juszczyk, K. Kamguyan, K. E. Jensen, G. Tosello and A. Boisen, *ACS Biomater. Sci. Eng.*, 2020, **6**, 2478–2486.
105 M. Dalskov Mosgaard, S. Strindberg, Z. Abid, R. Singh Petersen, L. Højlund Eklund Thamdrup, A. Joukainen Andersen, S. Sylvest Keller, A. Müllertz, L. Hagner Nielsen and A. Boisen, *Int. J. Pharm.*, 2019, **570**, 118658.
106 M. A. Rose, J. J. Bowen and S. A. Morin, *Chem. Phys. Chem.*, 2019, **20**, 909–925.
107 J. Kwon, E. Cheung, S. Park and M. Sitti, *Biomed. Mater.*, 2006, **1**, 216–220.
108 D. Naik, G. Balakrishnan, M. Rajagopalan, X. Huang, N. Trivedi, A. Bhat and C. J. Bettinger, *Adv. Sci.*, 2023, 2301084.
109 P. Glass, E. Cheung and M. Sitti, *IEEE Trans. Biomed. Eng.*, 2008, **55**, 2759–2767.
110 E. Buselli, V. Pensabene, P. Castrataro, P. Valdastri, A. Menciassi and P. Dario, *Meas. Sci. Technol.*, 2010, **21**, 105802.
111 M. R. Carvalho, J. P. S. Ferreira, D. A. Oliveira, M. P. L. Parente and R. M. Natal Jorge, *Numer. Methods Biomed. Eng.*, 2022, **38**(5), e3588.
112 M. L. Grivel and Y. Ruckebusch, *J. Physiol.*, 1972, **227**, 611–625.
113 D. Duchêne, F. Touchard and N. A. Peppas, *Drug Dev. Ind. Pharm.*, 1988, **14**, 283–318.
114 H. S. Ch'Ng, H. Park, P. Kelly and J. R. Robinson, *J. Pharm. Sci.*, 1985, **74**, 399–405.
115 B. S. Terry, A. B. Lyle, J. A. Schoen and M. E. Rentschler, *J. Biomech. Eng.*, 2011, **133**, 091010.
116 J. Wang, P. Wu, M. Liu, Z. Liao, Y. Wang, Z. Dong and X. D. Chen, *Food Funct.*, 2019, **10**, 2914–2925.
117 R. Deng, L. Pang, Y. Xu, L. Li, X. Wu and X. D. Chen, *Int. J. Food Eng.*, 2014, **10**, 645–655.
118 R. Deng, C. Selomulya, P. Wu, M. W. Woo, X. Wu and X. D. Chen, *Chem. Eng. Res. Des.*, 2016, **112**, 146–154.
119 P. Wu and X. D. Chen, *Curr. Opin. Food Sci.*, 2020, **35**, 10–19.
120 M. J. Ferrua and R. P. Singh, in *New Advances in Gastrointestinal Motility Research*, ed. L. K. Cheng, A. J. Pullan and G. Farrugia, Springer Netherlands, Dordrecht, 2013, vol. 10, pp. 243–266.
121 N. Palmada, J. E. Cater, L. K. Cheng and V. Suresh, *Fluids*, 2022, **7**, 40.
122 S. Babaee, Y. Shi, S. Abbasalizadeh, S. Tamang, K. Hess, J. E. Collins, K. Ishida, A. Lopes, M. Williams, M. Albaghdadi, A. M. Hayward and G. Traverso, *Nat. Mater.*, 2021, **20**, 1085–1092.
123 X.-G. Li, M. Chen, S. Zhao and X. Wang, *Stem Cell Rev. Rep.*, 2022, **18**, 2137–2151.
124 Y. Xiang, H. Wen, Y. Yu, M. Li, X. Fu and S. Huang, *J. Tissue Eng.*, 2020, **11**, 204173142096531.
125 D. P. Thomas, J. Zhang, N.-T. Nguyen and H. T. Ta, *Biosensors*, 2023, **13**, 136.
126 V. C. Ude, D. M. Brown, V. Stone and H. J. Johnston, *J. Nanobiotechnol.*, 2019, **17**, 70.
127 S. Y. Lee, Y. Lee, N. Choi, H. N. Kim, B. Kim and J. H. Sung, *BioChip J.*, 2023, **17**, 230–243.
128 J. McCright, A. Sinha and K. Maisel, *Cel. Mol. Bioeng.*, 2022, **15**, 479–491.
129 S. Walayat, A. J. Johannes, M. Benson, E. Nelsen, A. Akhter, G. Kennedy, A. Soni, M. Reichelderfer, P. Pfau and D. Gopal, *World J. Gastrointest. Endosc.*, 2023, **15**, 309–318.
130 E. A. Bonin, B. Verschoor, F. H. Silva, K. C. Vieira, S. K. Takata, E. A. Bonin, B. Verschoor, F. H. Silva, K. C. Vieira and S. K. Takata, *Advanced Endoscopy*, IntechOpen, 2019.
131 J. E. Lopera, M. A. de Gregorio, A. Laborda and R. Casta, *Int. J. Gastrointest. Interv.*, 2016, **5**, 138–148.
132 N. Gonzalo and C. Macaya, *Vasc. Health Risk Manage.*, 2012, **8**, 125–132.
133 B. D. Ulery, L. S. Nair and C. T. Laurencin, *J. Polym. Sci., Part B: Polym. Phys.*, 2011, **49**, 832–864.
134 G. G. Stefanini, R. A. Byrne, P. W. Serruys, A. de Waha, B. Meier, S. Massberg, P. Jüni, A. Schömig, S. Windecker and A. Kastrati, *Eur. Heart J.*, 2012, **33**, 1214–1222.
135 G. Balakrishnan, A. Bhat, D. Naik, J. S. Kim, S. Marukyan, L. Gido, M. Ritter, A. S. Khair and C. J. Bettinger, *Adv. Mater.*, 2023, **35**, 2211581.
136 A. P. Madrona, J. A. F. Hernández, M. C. Prats, J. R. Riquelme and P. P. Paricio, *Eur. J. Surg.*, 2000, **166**, 307–309.
137 M. Jurak, A. E. Wiącek, A. Ładniak, K. Przykaza and K. Szafran, *Adv. Colloid Interface Sci.*, 2021, **294**, 102451.
138 G. Enders, Gut: The Inside Story of Our Body's Most Underrated Organ (Revised Edition), Greystone Books Ltd, 2018.
139 L. W. Peterson and D. Artis, *Nat. Rev. Immunol.*, 2014, **14**, 141–153.
140 Microneedles for drug delivery and monitoring - ScienceDirect, **https://www.sciencedirect.com/science/article/abs/pii/B9780857096975500062**, (accessed 15 June 2023).
141 S. M. Bal, J. Caussin, S. Pavel and J. A. Bouwstra, *Eur. J. Pharm. Sci.*, 2008, **35**, 193–202.
142 G. Cummins, *Adv. Drug Delivery Rev.*, 2021, **177**, 113931.

143 L. T. Sørensen, U. Hemmingsen, F. Kallehave, P. Wille-Jørgensen, J. Kjærgaard, L. N. Møller and T. Jørgensen, *Ann. Surg.*, 2005, **241**, 654–658.
144 T. Fernandes, M. I. Oliveira, R. Castro, B. Araújo, B. Viamonte and R. Cunha, *Insights Imaging*, 2014, **5**, 195–208.
145 C. J. Bettinger, *Macromol. Biosci.*, 2011, **11**, 467–482.
146 T. R. Yeazel-Klein, A. G. Davis and M. L. Becker, *Adv. Mater. Technol.*, 2023, 2201904.
147 J. Kluin, H. Talacua, A. I. P. M. Smits, M. Y. Emmert, M. C. P. Brugmans, E. S. Fioretta, P. E. Dijkman, S. H. M. Söntjens, R. Duijvelshoff, S. Dekker, M. W. J. T. Janssen-van den Broek, V. Lintas, A. Vink, S. P. Hoerstrup, H. M. Janssen, P. Y. W. Dankers, F. P. T. Baaijens and C. V. C. Bouten, *Biomaterials*, 2017, **125**, 101–117.
148 S. P. Nikam, Y.-H. Hsu, J. R. Marks, C. Mateas, N. C. Brigham, S. M. McDonald, D. S. Guggenheim, D. Ruppert, J. I. Everitt, H. Levinson and M. L. Becker, *Biomaterials*, 2023, **292**, 121940.
149 R. Castro, D. Libânio, I. Pita and M. Dinis-Ribeiro, *WJG*, 2019, **25**, 777–788.
150 X. Chen, H. Yuk, J. Wu, C. S. Nabzdyk and X. Zhao, *Proc. Natl. Acad. Sci. U. S. A.*, 2020, **117**, 15497–15503.
151 S. Balamurugan, L. K. Ista, J. Yan, G. P. López, J. Fick, M. Himmelhaus and M. Grunze, *J. Am. Chem. Soc.*, 2005, **127**, 14548–14549.
152 B. Li, J. J. Whalen, M. S. Humayun and M. E. Thompson, *Adv. Funct. Mater.*, 2020, **30**, 1907478.
153 J. K. Park, K. Nan, H. Luan, N. Zheng, S. Zhao, H. Zhang, X. Cheng, H. Wang, K. Li, T. Xie, Y. Huang, Y. Zhang, S. Kim and J. A. Rogers, *Adv. Mater.*, 2019, **31**, 1905715.
154 A. Melocchi, M. Uboldi, N. Inverardi, F. Briatico-Vangosa, F. Baldi, S. Pandini, G. Scalet, F. Auricchio, M. Cerea, A. Foppoli, A. Maroni, L. Zema and A. Gazzaniga, *Int. J. Pharm.*, 2019, **571**, 118700.
155 R. Raman, T. Hua, D. Gwynne, J. Collins, S. Tamang, J. Zhou, T. Esfandiary, V. Soares, S. Pajovic, A. Hayward, R. Langer and G. Traverso, *Sci. Adv.*, 2020, **6**, eaay0065.
156 G. Balakrishnan, J. Song, C. Mou and C. J. Bettinger, *Adv. Mater.*, 2022, **34**, 2106787.
157 J. Zhang, G. Balakrishnan, S. Srinidhi, A. Bhat, S. Kumar and C. Bettinger, *Proceedings of the 20th ACM Conference on Embedded Networked Sensor Systems*, Association for Computing Machinery, New York, NY, USA, 2023, pp. 75–90.
158 J. Hughes and D. Rus, *2020 3rd IEEE International Conference on Soft Robotics (RoboSoft)*, 2020, pp. 836–843.
159 J. A. Shulgach, D. W. Beam, A. C. Nanivadekar, D. M. Miller, S. Fulton, M. Sciullo, J. Ogren, L. Wong, B. L. McLaughlin, B. J. Yates, C. C. Horn and L. E. Fisher, *Sci. Rep.*, 2021, **11**, 12925.

